RESEARCH ARTICLE

Short-Term Production Optimization for Electric Submersible Pump Lifted Oil Field With Parametric Uncertainty

NIMA JANATIAN [ID] **AND ROSHAN SHARMA**

Department of Electrical Engineering, Information Technology and Cybernetics, University of South-Eastern Norway, 3918 Porsgrunn, Norway

Corresponding author: Nima Janatian (nima.janatianghadikolaei@usn.no)

ABSTRACT This paper uses a scenario-based optimization method to address the Daily Production Optimization from an Electric Submersible Pump lifted oil field under the presence of uncertainty. The primary contribution of this work lies in addressing the presence of uncertainty in short-term production optimization of the oil industry, a significant aspect that is frequently overlooked. It has been shown that using the dynamic model of the plant in the optimization problem is too computationally expensive, even in a deterministic case. Therefore, the steady-state model of the system has been used in a robust optimization framework. The necessity of considering uncertainty in the optimization problem and the promising results of the proposed robust method is compared with the deterministic optimization counterpart. An additional novelty of this study involves the utilization of a scenario-based optimization framework to explore various forms of uncertainty, including uncertainty in well flow parameters and oil price. It has been shown that the uncertainty in oil price does not affect the optimal solution during normal operation, at least in short-term optimization such as Daily Production Optimization. On the contrary, the uncertainty in the well parameters is important to be considered since well flow parameters influence the optimizer in preferring one well over the other. Consequently, the economic objective for the lucrative business of the oil industry will be translated into production maximization, and the optimizer's task involves allocating the total production capacity among the different wells to maximize the proportion of the oil to water in the produced fluid.

INDEX TERMS Constrained optimization under uncertainty, electric submersible pump lifted oil well, parametric uncertainty, scenario-based robust optimization, short-term production optimization.

I. INTRODUCTION

The cost and revenue from an oil and gas production unit are typically affected by decisions that are required to be taken at different time scales. The planning horizon for these decisions ranges from seconds to the entire lifetime of the field, depending on the objectives. Daily Production Optimization (DPO), which is equivalent to Real-Time Optimization (RTO) from a process systems perspective, corresponds to the decisions and plans that are taken in the time scale of a few hours to a couple of days to maximize the daily operating

The associate editor coordinating the review of this manuscript and approving it for publication was Zhiwu Li [ID].

revenue of the production unit. Typical decisions in this scope involve selecting the choke opening of the different wells or allocating shared resources such as electric power and available lift gas in order to maximize the daily operational profit and ensure that the process and operating constraints are satisfied [1].

Daily production optimization has been reported to increase production by 1-4% [2], [3]. These improvements are even more pronounced for fields in the late plateau and decline phases than earlier phases [4]. On the other hand, it is well known that the presence of uncertainty may jeopardize the real-life application of constrained optimization since it is reasonably possible that the mismatch introduced

due to uncertainty may make an optimal solution practically infeasible. Thus, this paper will investigate the daily production optimization problem for an Electric Submersible Pump (ESP) lifted oil field under the presence of uncertainty.

A mathematical model for a single ESP oil well was developed in [5], and a linear Model Predictive Control (MPC) was designed in the Statoil Estimation and Prediction Tool for Identification and Control (SEPTIC) based on the step response model of the process. This controller was later implemented on a Programmable Logic Controller (PLC) in [6]. A Moving Horizon Estimator (MHE) was successfully implemented in [7] using the same model to estimate the flow rate and the productivity index of the well and the viscosity of the produced fluid.

A similar first principle model was derived in [8] for multiple ESP wells that share a common production manifold. The steady-state version of this model was used in [9] to develop a nonlinear optimization based on Sequential Quadratic Programming (SQP) for two optimal control strategies. The authors demonstrated that the production choke valve for each oil well has to be fully open during normal operation to maintain the optimal fluid flow rate and minimize electrical power. The same authors formulated a Mixed Integer Nonlinear Programming problem (MINLP) in [10] to calculate and identify the number of oil wells that should be used for special cases with low production demand. The dynamic version of the model was also used in [11], where the nonlinear model predictive control framework was implemented as an economic optimizer for maximizing profit. Even though the controls in this work were assumed constant throughout the prediction horizon, the length of the prediction horizon was limited to one second due to the fast dynamics of ESP and the high computational cost of a longer prediction horizon.

The research based on the model developed in [5] was pursued further, and it was shown in [12] that the linear model of an ESP lifted well varies significantly depending on the choke opening. Therefore, a model adaptation based on the homotopic transition between models was proposed in [13], where an adaptive linear MPC strategy was implemented as a Quadratic Dynamic Matrix Control (QDMC) algorithm in order to control the pump inlet pressure, minimizing the pump power and respecting the variable's constraints. An adaptive infinite horizon MPC strategy was also implemented in [14], where the proposed control law used successive linearization of the dynamic model in [5] to update the model internally. The ESP model was used in [15] to investigate the implementation aspects of measured disturbances in MPC. The main control objective in this work was to sustain a given production rate from the well while maintaining acceptable operating conditions for the pump.

A different approach was proposed in [1], translating the optimization objectives into control objectives to avoid solving a numerical optimization problem. The proposed method was applied to a single ESP lifted well successfully to track the inlet pressure of ESP subject to constraints. Nevertheless, the method violated the constraints dynamically. Recently a high-fidelity model of a single ESP well was proposed in [16] to be used as a surrogate model for the real plant. This model was used in [17] to propose an economic-oriented MPC auto-tuning strategy with a flexible structure able to enclose different MPC formulations, different tuning requirements, online implementation, and process attributes. An Echo State Neural Network was trained in [18] to capture the dynamic model of ESP well. The trained neural network was used for two nonlinear model predictive controllers that aimed to track the bottom-hole pressure subject to constraints on control inputs, bottom-hole and well-head pressures, and liquid flows.

The literature, as mentioned earlier, clearly shows two neglected aspects that are required to be addressed for the DPO problem for an ESP oil field:

- **Problem Formulation:** The control presented in [5] and almost all its successors aimed to track a certain set point (mostly bottom-hole pressure). This type of objective corresponds to the lower layer (Control and Automation layer as described in [4]) in the multilevel control hierarchy, where the set points to be tracked are determined by the higher-level optimizer called Production Optimization. Therefore, none of these works have answered the main question of DPO, which is: *How much should be produced from each well to maximize the economic objective?*

- **Parametric Uncertainty:** The other research works that started from [8] have considered multiple wells in a field, and the optimization problem is formulated to produce the optimal amount of fluid from each well to maximize the overall economic objective. Nevertheless, the composition of the produced fluid is considered constant over time, meaning the uncertainty in the real value of the well flow parameters like water cut or change in the water cut is neglected, while it is well known that the uncertainty in the parameter can make the optimal solution practically infeasible due to the mismatch between the prediction model and the real process [19], [20].

Therefore this paper aims to address these two knowledge gaps by investigating the daily production optimization from an ESP oil field with multiple oil wells considering the parameter uncertainty.

Scenario-based optimization method provides a versatile framework for robust optimization under uncertainty with improved conservativeness. The key feature of the method is the inclusion of finite realization of uncertainty represented by a scenario tree. The method was incorporated into a nonlinear model predictive control scheme in [21] for dynamic optimization of a semi-batch polymerization reactor under uncertainty. The method has been widely utilized across various applications. For instance, it has been applied to allocate pumped-storage hydropower units, as described in [22]. It was also used in the domain of oil production to optimally allocate a limited amount of available lift gas between multiple wells in a gas-lifted oil field [20], [23], [24]. However, using the dynamic model of ESP for DPO becomes problematic since the fast dynamics of the pumps require a

short sampling time, and the number of decision variables over a relatively long prediction horizon, such as in DPO, becomes intractable.

In order to address this problem, the piecewise steady operation of the plant is assumed throughout the prediction horizon. In particular, the fairly long prediction horizon of DPO is divided into segments, and the plant is considered to operate at a possibly new steady-state over each segment. Therefore, the steady-state model of the plant is used as the prediction model to determine the future of the system over each segment. This assumption is admissible not only because it is in line with the major conclusion of [4], which states that successive static optimization suffices in most relevant DPO cases, but also because the open loop simulation of the process demonstrates that the system is sufficiently fast that the transition between steady-states is negligible with respect to the length of the prediction horizon and can be overlooked.

Accordingly, the steady-state version of the model provided by [8] is used in this paper, supplemented by fairly subtle realistic assumptions and parametric uncertainty in various forms. The daily production optimization is formulated as successive scenario-based optimization problems in a receding horizon fashion to address the constraint fulfillment under the presence of uncertainty. In other words, only the first optimal decision is implemented in the plant, and the whole optimization process will be repeated at each time step. The main contribution of this work is threefold:

- Formulating the daily production optimization for an ESP-lifted oil field with a fairly more realistic objective function that includes the income from selling oil and the costs due to the electric power consumption, water treatment, and petroleum taxation.
- Considering the parametric uncertainty in DPO and using the scenario-based optimization framework to satisfy the fulfillment of the constraints robustly.
- Investigating the various forms of uncertainty, such as the uncertainty in oil price and the characteristics of the wells.

The rest of the paper is organized as follows. Section II briefly describes the mathematical modeling of the ESP oil field unit. The justification for preferring a steady-state model over a dynamic model is presented in Section III. Scenario-based optimization for DPO is presented in Section IV. The different aspects of the uncertainty, such as uncertainty in oil price and well parameters, are investigated in Section V before concluding in section VI.

II. MATHEMATICAL MODEL OF ESP-LIFTED OIL FIELD
A. PROCESS DESCRIPTION
An Electric Submersible Pump lifted oil well is an artificial lifting system where a submersible multistage centrifugal pump is installed at the bottom of the wellbore [8] to produce the pressure gradient needed for flowing the fluid to the surface. ESP lifting method is well suited for producing high volumes of heavy liquid [25]. Fig. 1 demonstrates the
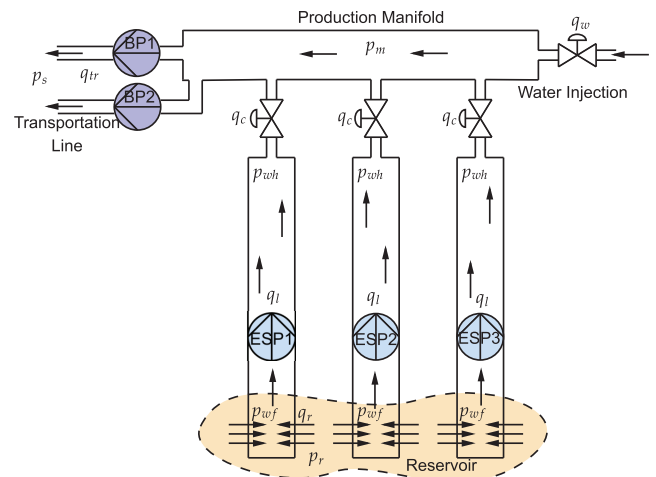
FIGURE 1. Schematic diagram of the production network with three ESP lifted oil wells and two identical transportation lines.

schematic diagram of the considered production network in this paper with three oil wells. Each well is equipped with an ESP unit at the bottom hole and a production chock valve at the wellhead. The amount of fluid produced from each well can be controlled by manipulating the speed of the pump. The oil produced from each well is collected together in a common production manifold. The reservoir is assumed to contain two-phase fluid, including crude oil with higher viscosity and water with no gas flow. The viscosity of the fluid produced from the wells is reduced by adding water to the production manifold from one end using a water injection valve to ease the transportation of the highly viscous fluid over a long distance. Two identical transportation lines are used to transport the gathered fluid from the production manifold to the separator located on the topside facility. Each transportation line is fitted with a booster pump which is used to increase the pressure to overcome the sum of flowing pressure losses in the transportation line.

Simple mechanistic models of ESP-lifted oil wells are developed in [5] and [8] for optimization and control purposes. Both models are derived based on mass and momentum balance in the pipes and manifolds. The considered mathematical model of this paper is adopted from [8] with subtle modifications on assumptions:

- Modeling the electrical motors subsystem is neglected due to the fast response of electrical systems.
- Assumption of constant water cut in the production manifold is substituted by a more realistic one. Therefore, instead of injecting water to keep the water cut constant, which needs a perfect controller, a constant flow of water is injected into the manifold. Accordingly, the water cut of the liquid phase within the manifold is varying and depends on the proportion of fluid produced from production chock valves.
- Water cuts of the wells are considered to be different to draw a meaningful optimization problem.

B. GOVERNING EQUATIONS

This section only briefly presents the governing equations of the process since modeling is not the main focus and contribution of this work. However, the readers are referred to [8] for a more detailed explanation of the modeling.

The process is described by three states for each well, namely, the pressure at the bottom hole p_b^i, the pressure at the wellhead p_h^i, and the average volumetric flow rate of the well q_l^i, where the superscript i refers to the ith oil well. The remaining states are the pressure in the production manifold p_m and the average volumetric flow rate of the jth transportation line q_{tr}^j. The corresponding differential equations are given by:

$$\dot{p}_b^i = \frac{\beta}{A_r^i L_r^i}\left[q_r^i - q_l^i\right] \tag{1}$$

$$\dot{p}_h^i = \frac{\beta}{A_t^i L_t^i}\left[q_l^i - q_c^i\right] \tag{2}$$

$$\dot{q}_l^i = \frac{A_t^i}{\rho_l^i\left(L_r^i + L_t^i\right)}\left[p_b^i - p_h^i + \rho_l^i g H_{esp}^i(q_l^i, f^i)\right.$$
$$\left. - \rho_l^i g(L_r^i + L_t^i) - \Delta p_{f,t}^i - \Delta p_{f,r}^i\right] \tag{3}$$

$$\dot{p}_m = \frac{\beta}{A_m L_m}\left[\sum_{i=1}^{3} q_c^i - \sum_{j=1}^{2} q_{tr}^j + q_w^{inj}\right] \tag{4}$$

$$\dot{q}_{tr}^j = \frac{A_{tr}^j}{\rho_{tr}^j L_{tr}^j}\left[p_m - p_s + \Delta p_{bp}^j - \Delta p_{f,tr}^j\right] \tag{5}$$

And the set of algebraic equations is given by:

$$q_r^i = \text{PI}^i\left(p_r - p_b^i\right) \tag{6}$$

$$q_c^i = C_v^i\sqrt{\frac{\max(p_h^i - p_m, 0)}{\rho_l^i}} \tag{7}$$

$$\Delta p_f^i = \frac{f_D L \rho v^2}{2D_h} \tag{8}$$

$$H_{esp}^i(Q, f) = \frac{\bar{a}_0^i}{f_0^2}f^2 + \frac{\bar{a}_1^i}{f_0}fQ(f) + \bar{a}_2^i Q^2(f) + \frac{\bar{a}_3^i}{f}f_0 Q^3(f) \tag{9}$$

$$\text{BHP}_{esp}^i(Q, f) = \frac{\hat{a}_0^i}{f_0^3}f^3 + \frac{\hat{a}_1^i}{f_0^2}f^2 Q(f) + \frac{\hat{a}_2^i}{f_0}fQ^2(f)$$
$$+ \hat{a}_3^i Q^3(f) + \frac{\hat{a}_4^i}{f}f_0 Q^4(f) \tag{10}$$

$$\rho_l^i = \text{WC}^i\rho_w + (1 - \text{WC}^i)\rho_o \tag{11}$$

$$\text{WC}_{tr} = \frac{q_w^{inj} + \sum_{i=1}^{3} \text{WC}^i q_c^i}{q_w^{inj} + \sum_{i=1}^{3} q_c^i} \tag{12}$$

$$q_o = \sum_{j=1}^{2}(1 - \text{WC}_{tr})q_{tr}^j \tag{13}$$

TABLE 1. List of the algebraic variables and parameters.

Variable	Description
q_r	Volumetric flow rate from reservoir into well
q_c	Volumetric flow rate through production choke valve
ρ_l	Density of the fluid in the well
H_{esp}	Head developed by ESP
BHP_{esp}	ESP brake horsepower
Δp_f	Frictional pressure drop in the pipe
WC_{tr}	Water cut in transportation line
WC	Water cut of the well
PI	Productivity index of the well
q_o	Total produced oil
q_w	Total produced water
$Q_{\min}$	Minimum flow through the ESP
$Q_{\max}$	Maximum flow through the ESP

TABLE 2. List of the parameters and their corresponding values.

Parameter	Value	Unit	Comments
L_{tr}	4000	[m]	Length of transportation line
L_m	500	[m]	Length of production manifold
L_t	2000	[m]	Length of well above ESP
L_r	100	[m]	Length of well below ESP
D	0.1569	[m]	Diameter of all pipelines
A	0.0193	[m^2]	Cross section area of all pipelines
β	1.5e9	[N/m^2]	Bulk modulus of the reservoir fluid
ρ_o	900	[kg/m^3]	Density of water
ρ_w	1000	[kg/m^3]	Density of oil
p_r	220	[bar]	Pressure of the reservoir
p_s	30	[bar]	Pressure of the separator
C_v	0.2275	$\left[\sqrt{\frac{\text{kgm}^3}{\text{s}^2\text{bar}}}\right]$	Valve opening characteristic
μ_o	100e-6	[m^2/s]	Kinematic viscosity of oil
μ_w	1e-6	[m^2/s]	Kinematic viscosity of pure water
Δp_{bp}	10	[bar]	Pressure gradient by booster pump
f_0	60	[Hz]	ESP characteristics ref. freq.
$Q_{f_0,\min}$	228.648	[gpm]	ESP minimum flow at ref. freq.
$Q_{f_0,\max}$	400.111	[gpm]	ESP maximum flow at ref. freq.

$$q_w = \sum_{j=1}^{2} \text{WC}_{tr} q_{tr}^j \tag{14}$$

$$Q_{\min}^i(f) = \frac{f}{f_0}Q_{f_0,\min}^i \tag{15}$$

$$Q_{\max}^i(f) = \frac{f}{f_0}Q_{f_0,\max}^i \tag{16}$$

All the algebraic variables of the model are introduced in Table 1, and the model parameter values are presented in Table 2. The Darcy friction factor f_D in (8) can be evaluated using Serghides' explicit approximation to Colebrook-White equation [26]. The polynomial coefficients of ESP in (9) and (10) are also presented in Table 3.

Note that the algebraic variables can be easily substituted in the differential equations of the model presented in (1) to (5) to obtain an explicit set of ordinary differential

TABLE 3. Polynomial coefficients of ESP.

	$\bar{a}_0 \backslash \hat{a}_0$	$\bar{a}_1 \backslash \hat{a}_1$	$\bar{a}_2 \backslash \hat{a}_2$	$\bar{a}_3 \backslash \hat{a}_3$	$\bar{a}_4 \backslash \hat{a}_4$
H_{esp}	3.9719e3	-9.4149	4.5285e-2	-8.6465e-5	0
BHP_{esp}	2.2498e2	7.3984e-1	-6.8839e-4	2.1777e-6	-5.4696e-9

TABLE 4. Nominal values of uncertain parameters.

Parameter	Well 1	Well 2	Well 3	Unit
PI_{nom}	4.5e-4	5.4e-4	4.1e-4	$\left[\frac{m^3}{bar.s}\right]$
WC_{nom}	0.23	0.05	0.67	-

equations (ODE) in a compact form as:

$$\dot{x} = f(x, u, d) \tag{17}$$

where $x \in \mathbb{R}^{12}$ and $u \in \mathbb{R}^3$ are the states and system inputs, and $d \in \mathbb{R}^6$ is the vector of the uncertain parameters of the process as given by:

$$\begin{bmatrix} \mathbf{p_b} & \mathbf{p_h} & \mathbf{q_l} & \mathbf{p_m} & \mathbf{q_{tr}} \end{bmatrix} \tag{18}$$

$$\begin{bmatrix} f^1 & f^2 & f^3 \end{bmatrix} \tag{19}$$

$$\begin{bmatrix} PI^1 & PI^2 & PI^3 & WC^1 & WC^2 & WC^3 \end{bmatrix} \tag{20}$$

C. UNCERTAINTY DESCRIPTION

The uncertainty in the productivity index and water cut of the wells are considered in this study. The productivity index PI represents the reservoir's ability to deliver fluids to the wellbore, and the water cut WC is defined as the volumetric flow rate of water to the total produced liquid. For a network with three oil wells, there exist six uncertain parameters in the problem. Amongst specialists in the field, it is widely acknowledged that the water cut is more prone to experiencing abrupt changes, whereas alterations in the productivity index occur in a smoother manner. Hence, it is reasonable to suppose that the quantification of uncertainty in the water cut is greater than the uncertainty in the productivity index. As a result, a deviation of $\pm 10\%$ and $\pm 30\%$ from their nominal values are considered for PI and WC of each oil well, respectively, and the parameters can take any value within their bounds. No specific distribution of the parameters is selected to challenge the controller; thus, all the values in the uncertainty region are equally likely to occur. The nominal values of the parameters and their upper and lower bounds are presented in Table 4.

III. DYNAMIC VERSUS STEADY-STATE OPTIMIZATION

Although it has been argued in [4] that repetitive static optimization formulation suffices in most relevant DPO cases, some effort has been made to integrate the DPO layer into the Control and Automation layer using multistage nonlinear model predictive control with economic objective function as a dynamic optimizer in [20], [23], and [24]. Accordingly, this section intends to illustrate why the same approach is not applicable, particularly to the ESP lifted oil field described in Section II.

To do so, a deterministic nonlinear MPC is considered with an economic objective function to maximize the profit from the field. The primary objective is to adjust the pump frequencies in order to produce an optimal amount of fluid from each well for a given separator capacity. Therefore, the objective function includes the total income from selling the

produced oil with a negative sign to pose it as a minimization problem. Additionally, the costs due to electric power consumption of the ESPs, water treatment, and carbon taxation are incorporated into the objective function. Hence over the prediction horizon with the length N_p the objective function is given by:

$$J_{eco} = \sum_{k=1}^{N_p} \left(-c_o q_o^k + c_e \sum_{i=1}^{3} BHP_{esp}^{i,k} + c_s q_w^k + c_t q_o^k \right) \tag{21}$$

where c_o, c_e, c_s, and c_t denote the price of oil, electricity, water treatment, and carbon taxation, respectively. Their values are presented in Table 5.

The most important operational constraints in the problem arise from separator capacity and the ESP operating envelope. In particular, the magnitude of produced fluid (mixture of oil and water) should be equal to or less than the separator handling capacity, and the ESP pumps need to be kept within a safe operating window to avoid mechanical failure. Thus, the optimal control problem formulation over the prediction horizon is given by:

$$\min_{x,u} J_{eco}(x, u, d) \tag{22a}$$

$$\text{s.t. } x_k = f(x_{k-1}, u_{k-1}, d), \quad k = 1, \dots, N_p \tag{22b}$$

$$\sum_{i=1}^{2} q_{tr}^{i,k} \leq Q_{sep}^k, \quad k = 1, \dots, N_p \tag{22c}$$

$$Q_{min}^{i,k} \leq q_l^{i,k} \leq Q_{max}^{i,k}, \quad k = 1, \dots, N_p \tag{22d}$$

$$u_{LB} \leq u_k \leq u_{UB}, \quad k = 0, \dots, N_p - 1 \tag{22e}$$

$$\Delta u_{LB} \leq \Delta u_k \leq \Delta u_{UB}, \quad k = 0, \dots, N_p - 1 \tag{22f}$$

Equation (22b) denotes the discretized dynamic model and is imposed as a state continuity constraint. The constraint on the total produced fluid is enforced in (22c), where Q_{sep}^k stands for the maximum handling capacity of the separator. The safe operation of the ESP pumps within the pump envelope is denoted in (22d) by maintaining the pump flow between the minimum and maximum allowed flow which is provided by (15) and (16). The lower and upper bounds on the control signal (pump frequency) and the rate of change of control inputs are also implemented in (22e) and (22f), respectively.

The optimal control problem in (22) is solved in a receding horizon fashion using the nominal value of the parameters provided in Table 2 and Table 3. A sampling time of 0.3 seconds and a prediction horizon of 25 time steps (7.5 s) is used. The separator capacity is considered to be 8500 $[m^3/d]$. The lower bound and upper bound for pump frequency is 45 and 80 [Hz]. The rate of change in pump frequency has to be maintained between -1 and 1 [Hz/s]. The prices in the objective function are presented in Table 5. The dynamic optimization problem is discretized using the direct multiple shooting method in CasADi v.3.5.5. The simulations are implemented in MATLAB R2022b, and IPOPT v.3.14.1 solver has been used to solve the optimization problems.

TABLE 5. Prices.

Price	Value	Unit	Comments
c_o	75	[\$/bbl]	Price of oil per barrel
c_e	15	[\$/kWh]	Price of electricity per unit of energy
c_s	2	[\$/bbl]	Cost of water treatment per barrel
c_t	30	[\$/bbl]	Carbon taxation per barrel

The simulation result is presented in Fig. 2. All the constraints on the control input, separator capacity, and pump envelope are respected successfully, as demonstrated in subplots (a), (b), and (e). However, the execution time remains the main challenge for dynamic optimization. The execution time, which is shown in subplot (d), has an average of 0.15 s and peaks up to 0.2 s at some points. This simply means that the method is barely implementable even in a deterministic case since the computations should be executed during one sampling time (0.3 s). It is also worth mentioning that the uncertainty is not considered yet, and the prediction horizon is relatively short. Considering uncertainty with scenario-based dynamic optimization problem increases the execution time significantly and may become intractable if more oil wells are considered in the field, as observed in [20], [23], and [24]. Therefore, using a steady-state model is unavoidable for DPO under uncertainty, and it is in line with the claim in [4], which states that a steady-state model typically suffices for DPO.

IV. SCENARIO-BASED OPTIMIZATION USING STEADY-STATE MODEL

According to the scenario-based optimization approach, the uncertainty region is discretized into finite distinct possible realizations, and the system's evolution is evaluated based on a scenario tree. This means that the future evolution of the plant is branched into different trajectories depending on which realization of the uncertainty occurs in reality. Nevertheless, the computations may become intractable since the number of scenarios grows exponentially with the number of considered uncertainty and the length of the prediction horizon. The solution to this drawback gives rise to a concept named robust horizon. The robust horizon means the branching is continued for only a certain number of samples which is typically one or two samples ahead in time. The justification for a robust horizon arises from the fact that the corresponding control variables and state trajectories will be recalculated and refined in future sampling times; hence, the far future uncertainty does not need to be represented precisely.

Considering the maximum and minimum values of the six uncertain parameters and the nominal case, $N_s = 2^6 + 1 = 65$ possible realizations for uncertainties or branches are considered in this paper, including all the combinations of boundary values and the nominal case. The scenario tree with the robust horizon $N_r = 1$ is exhibited in Fig. 3. Each path from the root node to the leaf is called a scenario; thus, the method is also known as scenario-based optimization.

It is worthwhile to mention that this formulation imposes an extra constraint which is known as a non-anticipativity
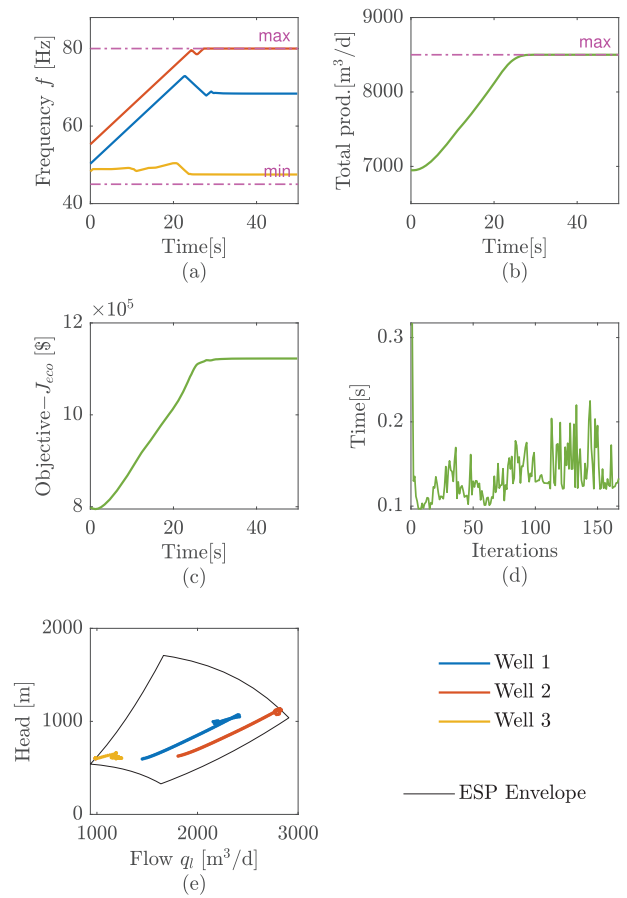

FIGURE 2. Dynamic optimization using standard deterministic Nonlinear Model Predictive Control: (a) Pump frequency, (b) Total produced fluid, (c) Negative of the objective function, (d) Execution time, (e) ESP operating envelope.
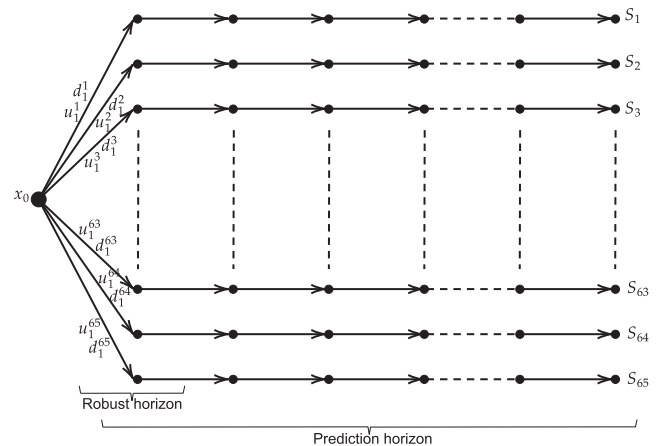

FIGURE 3. Scenario tree with $N_s = 65$ scenarios and robust horizon $N_r = 1$.

constraint. This constraint represents the fact that in real-time decision-making, the controller can not anticipate the future realization of the uncertainty. Therefore, all the controls that branch from a parent node are made equal using the non-anticipativity constraint.

Once the scenario tree and its prerequisites have been defined, the objective function of each scenario j can be calculated as:

$$J_{eco}^{j} = \sum_{k=1}^{N_p} \left(-c_o q_o^{k,j} + c_e \sum_{i=1}^{3} \text{BHP}_{esp}^{i,k,j} + c_s q_w^{k,j} + c_t q_o^{k,j} \right) \tag{23}$$

Accordingly, the optimization problem can be formulated over all the discrete scenarios of the scenario set $\mathcal{S} = \{1, \ldots, N_s\}$, throughout the prediction horizon $\mathcal{K} = \{1, \ldots, N_p\}$ as follows:

$$\min_{\mathrm{x,u}} \sum_{j=1}^{N_s} \omega_j J_{eco}^{j} \tag{24a}$$

$$\text{s.t.} \ f\left(x_k^j, u_k^j, d_k^j\right) = 0, \ \forall k \in \mathcal{K}, \ \forall j \in \mathcal{S} \tag{24b}$$

$$\sum_{i=1}^{2} q_{tr}^{i,k,j} \leq Q_{\text{sep}}^k, \ \forall k \in \mathcal{K}, \ \forall j \in \mathcal{S} \tag{24c}$$

$$Q_{\text{min}}^{i,k,j} \leq q_l^{i,k,j} \leq Q_{\text{max}}^{i,k,j}, \ \forall k \in \mathcal{K}, \ \forall j \in \mathcal{S} \tag{24d}$$

$$u_{LB} \leq u_k^j \leq u_{UB}, \ \forall k \in \mathcal{K}, \ \forall j \in \mathcal{S} \tag{24e}$$

$$u_k^j = u_k^l \ \text{ if } \ x_k^{p(j)} = x_k^{p(l)}, \ \forall k \in \mathcal{K}, \ \forall j \& l \in \mathcal{S} \tag{24f}$$

where J_{eco}^{j} is the objective function of the jth scenario and ω_j is the corresponding tuning weight that reflects the relative likelihood of occurring j^{th} scenario. The steady-state condition of the system is implemented as a constraint in (24b). It ensures that the states at every time $k \in \mathcal{K}$ from scenario j are at a steady condition which is a function of their corresponding control u_k^j and uncertainty realization d_k^j. The constraints on the separator capacity, pump envelope, and frequency are imposed in (24c), (22d), and (24e), respectively. It should be noted that the constraint on the change of control input is not relevant anymore since the transition between the steady-states is neglected. Instead, the non-anticipativity constraint is introduced in (24f), which reflects the fact that at each time step k, controls u_k^j and x_k^l from scenarios j and l with the same parental node $x_k^{p(j)} = x_k^{p(l)}$ have to be equal. In other words, all the controls that are branched from the same parental node are equal. It should be noted that, as shown in Fig. 3, branching has been done only for the first sampling time. Therefore, $u_1^1 = u_1^2 = \ldots = u_1^{64} = u_1^{65}$ is the only set of non-anticipativity constraints in the problem, and according to the receding horizon strategy, this first control action is the one that will be applied to the real system. Hence, the non-anticipativity constraint guarantees that this value is unique.

A comparison between the proposed scenario-based optimization method and a deterministic standard optimization is conducted to demonstrate the capability of the method to handle uncertainty. To this end, a deterministic nonlinear MPC controller is also designed based on the steady-state model with nominal values of uncertain parameters. The formulation is not duplicated since it can be considered as

a special case of the optimization problem in (24) with only one nominal scenario.

A prediction horizon of two days with a sampling time of six hours is chosen for the controller. The plant containing well flow characteristic uncertainty is simulated using both deterministic and scenario-based methods. The simulation results are presented in Fig. 4 and Fig. 5. Subplots (b) and (c) in Fig. 4 demonstrate that for some realizations of uncertainty, the constraints on separator capacity and pump envelope will be violated. This means the lower-level controller will be requested to track infeasible set points due to neglecting the uncertainty in the optimization problem. On the other hand, the scenario-based method, as can be seen from subplots (b) and (c) in Fig. 5, successfully satisfies all the constraints for all realization of the uncertainty within the considered uncertainty range. Two important points should be noted. First, like any other robust method, the scenario-based method is not able to cope with uncertainty beyond the considered range of uncertainty. Second, the capability of compensation for uncertainty is not free. The price that should be paid to gain this robustness is sacrificing optimality to some extent. In this sense, the sacrifice means that the optimizer decides to produce less than the maximum allowed production, shown in a thick red line in subplot (b), to ensure that the upper bound of constraint will be respected for all uncertainty realizations. It should be noted that the execution times for both cases, as presented in Table 6, are in the order of seconds, which means using the steady-state model allowed the computations to be executed safely within the sampling time (six hours). Hence, the solution can be implemented easily.

V. VARIOUS FORMS OF UNCERTAINTY
Using scenario-based optimization with the steady-state version of the model for prediction provides the possibility to consider different types of uncertainty in the optimization problem. Consequently, this section investigates how uncertainty in oil price and well characteristics affects daily production optimization problems.

A. UNCERTAINTY IN OIL PRICE
Two simulation cases are proposed to study the effect of uncertainty on the oil price. In the first case, the optimization problem defined in (24) is solved and applied to a plant considering the oil price is constant at 75 [\$/bbl], as presented in Table 5. For the second simulation case, the oil price is assumed to fall drastically from almost 110 [\$/bbl] to 60 [\$/bbl] as shown in subplot (f) in Fig. 6. In this case, the average of maximum and minimum oil prices shown by the black line (real price) in subplot (f) is considered to calculate the objective function.

The simulation results for both cases are plotted in Fig. 6. The optimal frequency of the pumps for both constant and varying scenarios are demonstrated in subplots (a) and (b), respectively. It can be seen that despite the difference between oil prices, the optimal frequencies for the two cases are the same. As a result, the total produced fluid for both cases
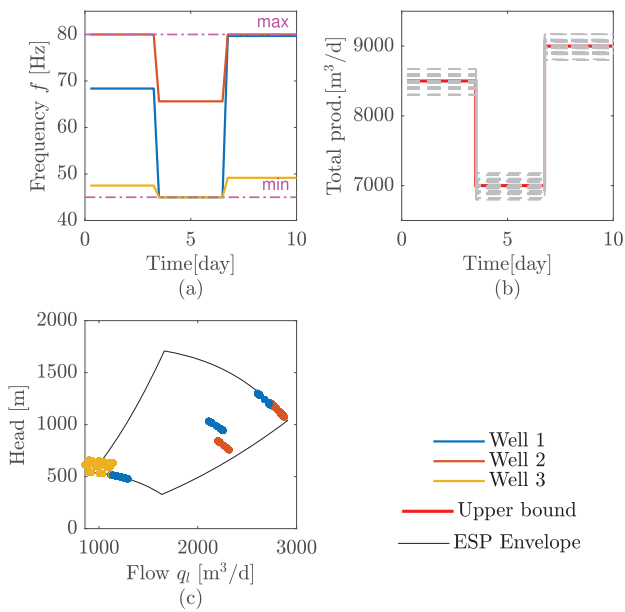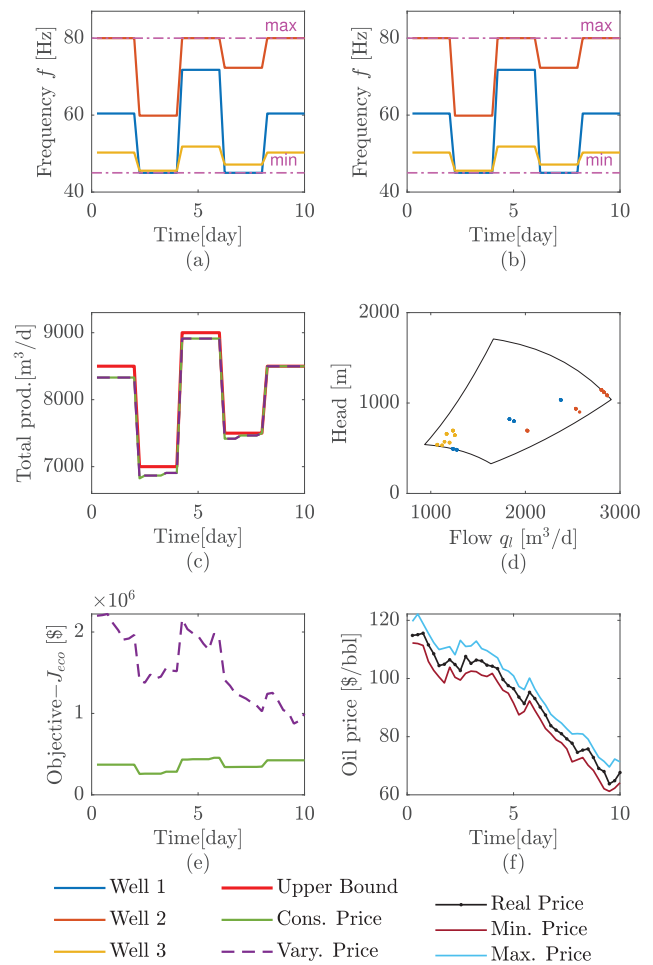
FIGURE 4. Deterministic DPO based on nominal values of the parameters applied to the uncertain model: (a) Pump frequency, (b) Total produced fluid, (c) ESP operating envelope.
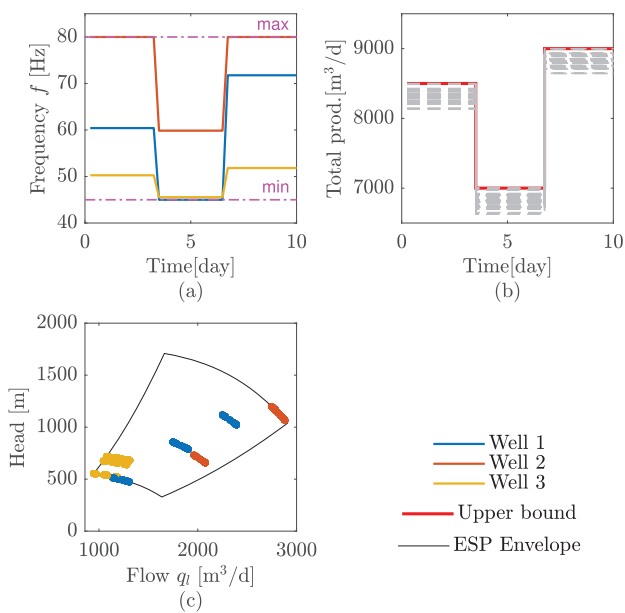
FIGURE 5. Scenario-based DPO based on scenario tree applied to the uncertain model: (a) Pump frequency, (b) Total produced fluid, (c) ESP operating envelope.


FIGURE 6. Scenario-based DPO based on constant and varying oil price: (a) Pump frequency for constant oil price case, (b) Pump frequency for varying oil price case, (c) Total produced fluid for both cases, (d) ESP operating envelope for both cases, (e) Negative value of the objective functions for both cases, (f) Variation of the oil price for the varying price case.

is the same, as presented in subplot(c), together with the separator capacity for handling the production in a solid red line. However, the absolute values of the objective functions, as depicted in subplot (e), are different due to the difference between oil prices in the two cases. This implies that the optimal solution for both cases is identical. In other words, although the absolute values of the objective functions are different, the uncertainty in oil price does not influence the optimal solution itself. Hence, the uncertainty in oil price

does not affect the short-term optimization from ESP lifted field.

Another case study is conducted where the oil price drops even more to almost 20 [$/bbl] to demonstrate that the economic optimizer works appropriately. The simulation result is presented in Fig. 7. Subplot (b) clearly shows that in the beginning, the optimizer tries to produce as much as possible while respecting the upper bound of the production constraint. However, after 7.75 days, it decides to decrease the production rate. The reason can be explained by taking a closer look at the negative value of the objective function and the oil price in subplots (c) and (d). It can be seen that after 7.75 days, when the oil price drops approximately from 37 [$/bbl] to 34 [$/bbl], the objective function changes sign. In other words, production from the field is not profitable anymore. As a result, the optimizer decides to set the frequency of all pumps to the minimum value, as shown in subplot (a), to decrease production and financial loss.

Furthermore, it is important to mention that the execution times for all cases, as shown in Table 6, are in the range of
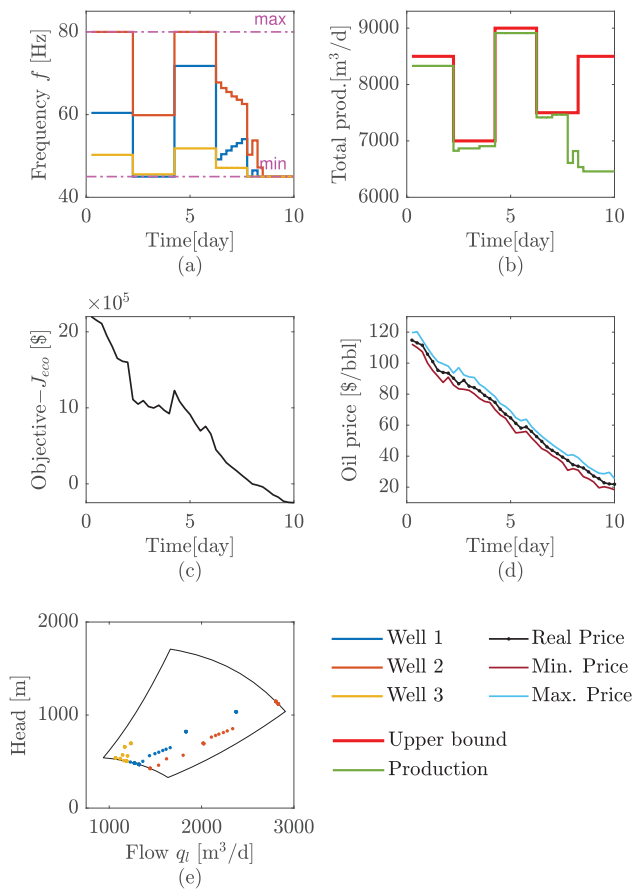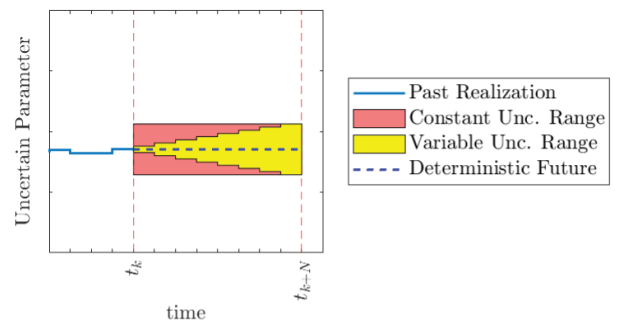
FIGURE 7. Scenario-based DPO for significantly low oil price: (a) Pump frequency, (b) Total produced fluid and maximum allowed production, (c) Negative value of the objective function, (d) Variation of the oil price, (e) ESP operating envelope.
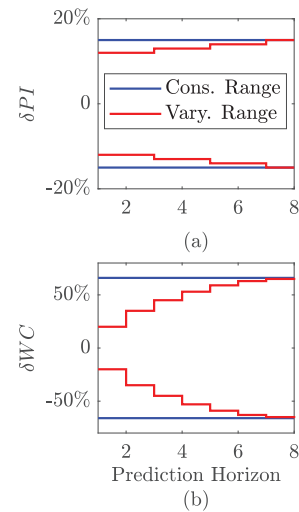

FIGURE 8. Schematic illustration of the constant and varying range of uncertainty for an uncertain parameter over the prediction horizon.
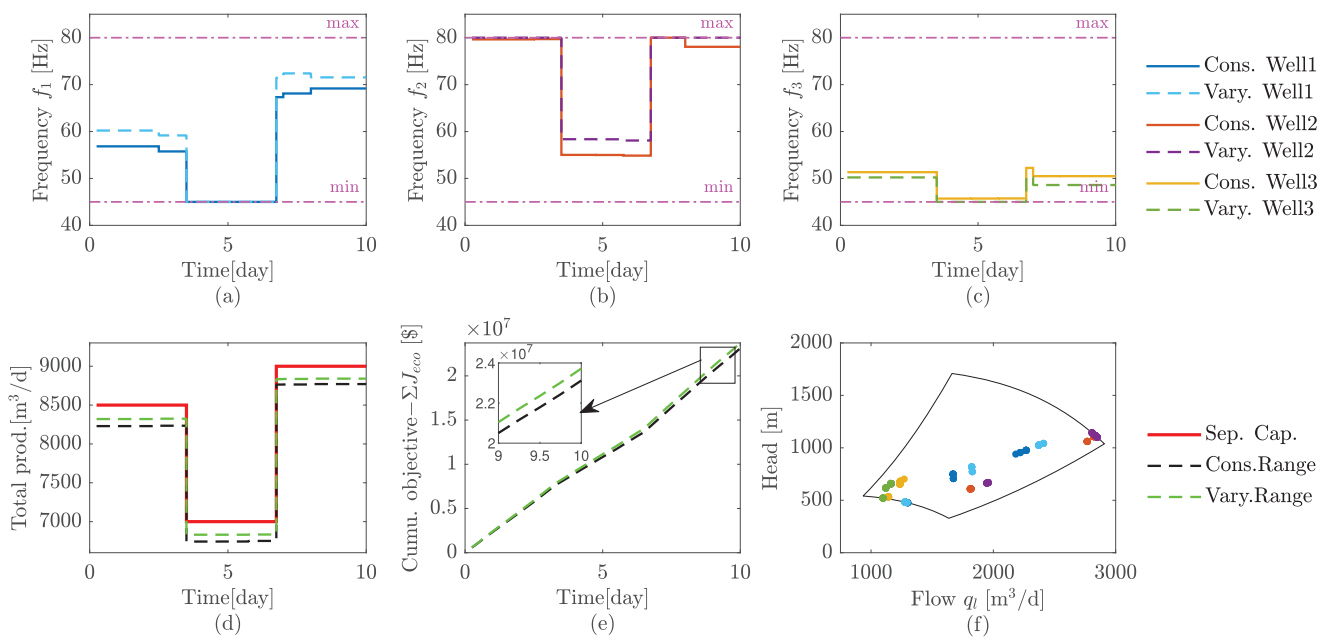

FIGURE 9. The constant and varying range of the uncertainty considered for all the wells: (a) Productivity index, (b) Water cut.

TABLE 6. Execution time of different simulation cases.

Simulation case	mean [s]	max [s]	Corresponding Fig.
Deterministic MPC	0.0122	0.0278	Fig. 4
Multistage MPC	1.0494	2.0635	Fig. 5
Varying price scenario	1.0026	1.8021	Fig. 6
Constant price scenario	0.8918	1.5027	Fig. 6
Low price scenario	1.3749	2.3056	Fig. 7
Constant uncertainty range	0.9805	1.9656	Fig. 10
Varying uncertainty range	1.1156	2.0350	Fig. 10

seconds, and implementing the solution should be straightforward.

B. UNCERTAINTY IN WELL CHARACTERISTICS

An additional prospect worth exploring is how the variation in uncertainty range can be exploited to decrease the conservativeness of the method. To illustrate it more, consider a single bounded slightly varying uncertain parameter over the prediction horizon as shown in Fig. 8. The idea is to exploit the fact that uncertainty grows in the future to decrease the conservativeness of the method. In other words, although the uncertain parameter can take an extreme value in the future, this extreme value necessarily does not occur at the moment. This is the case, especially for the daily production optimization of an ESP network. For example, the uncertainty in the water cut of oil well over the prediction horizon with a length of 2 days and a sampling time of 6 hours. The water cut may increase or decrease by 50% over the course of two days; however, this change may not occur at once. Therefore it makes sense to assume that uncertainty during the next six hours is limited to ±15% of nominal value, and it increases gradually to ±50%.

Two simulation cases have been considered to demonstrate the concept. In the first case, namely the constant range scenario, there is a constant ±15% and ±65% uncertainty in the productivity index and water cut of all wells, respectively, throughout the prediction horizon. However, in the varying range scenario, as shown in Fig. 9, it has been assumed that the uncertainty in the productivity index grows gradually from ±12% to ±15% and uncertainty in the water cut grows gradually from ±20% to ±65%. The simulation result for two cases is presented in Fig. 10. For both cases, the pump frequency of the three pumps is demonstrated in subplots (a), (b), and (c), respectively. It can be seen from subplot (d) that the difference between frequencies resulted in a higher production rate for the varying range scenario, which is

FIGURE 10. Scenario-based DPO based on the constant and varying range of uncertainty in the well parameters: (a) Pump frequency of ESP1, (b) Pump frequency of ESP2, (c) Pump frequency of ESP3, (d) Total produced fluid, (e) Negative value of the cumulative objective function, (f) ESP operating envelope for both cases.

equivalent to a 2.58% increase in the cumulative objective function, as shown in subplot (e). Additionally, as presented in Table 6, the execution times are not more than two seconds, which means the solution is implementable.

VI. CONCLUSION

This paper exploited the scenario-based optimization method to address the Daily Production Optimization for an ESP lifted oil field under parametric uncertainty. It was shown that using a steady-state model in the context of DPO for an ESP lifted oil field is tractable and has a huge potential to be used in a real oil field.

The accomplishment of the proposed method and the necessity of considering uncertainty is demonstrated by a comparison between the deterministic optimization based on a nominal model and the scenario-based optimization applied to a plant containing uncertainty. It has been shown that scenario-based optimization for DPO yields a robust solution, and safe operation of the ESP pump as well as robust satisfaction of the operational constraints, are guaranteed.

The potentials provided by representing the uncertainty with a scenario tree were exploited to investigate the different forms of uncertainty. It has been shown that the uncertainty in the oil price does not affect the short-term optimal production, at least during the normal operation of the market. Additionally, it has been demonstrated that for the DPO solution to be affected by the oil price, there has to be an extremely low price for the oil, which is not impossible but relatively rare during normal operation. Nevertheless, if such a rare occasion occurs, DPO can handle the situation by minimizing production from the field. This implies an intuitive and yet

interesting conclusion, that is, the economic objective would be translated to achieving either maximum or minimum production, depending on whether the production is profitable or not.

On the other hand, the investigation on the range of considered uncertainty in well flow parameters revealed that contrary to the oil price, the uncertainty related to the well characteristics is significantly important, and the net profit from a field can be increased by reducing the uncertainty in well flow parameters. This observation can be easily explained by considering that during the regular operation of a lucrative business such as oil production, the economic objective is typically equivalent to maximizing the total production from the field. Consequently, the daily production optimization seeks to allocate this total production among the different wells in a way that maximizes the proportion of the oil to water in the total produced fluid, which is a direct outcome of the well parameters.

In summary, this research yields two key findings. Firstly, utilizing scenario-based optimization effectively manages uncertainty in daily production optimization. This is crucial because deviating from optimal pump operation reduces their lifespan and entails costly repairs. Secondly, while price uncertainty can be disregarded in short-term optimization, it is vital to account for uncertainties in well characteristics.

Although this paper discusses several useful outcomes of the proposed method, there are potential opportunities for further improvement yet to be explored. First, the dynamic measurements that are being obtained continuously in a real-time application can be used together with estimation algorithms to truncate the range of uncertainty and potentially

improve the method in terms of conservatives. Second, the method can be extended using Mixed Integer Optimization, which makes it possible to shut down the wells, if it is necessary, in a more complex network with more oil wells.

REFERENCES

[1] D. Krishnamoorthy, K. Fjalestad, and S. Skogestad, "Optimal operation of oil and gas production using simple feedback control structures," *Control Eng. Pract.*, vol. 91, Oct. 2019, Art. no. 104107, doi: 10.1016/j.conengprac.2019.104107.

[2] B. Stenhouse, M. Woodman, and P. Griffiths, "Model based operational support—Adding assurance to operational decision making," presented at the SPE Intell. Energy Conf. Exhib., Mar. 2010, Paper no. SPE-128694-MS, doi: 10.2118/128694-MS.

[3] A. F. Teixeira, M. C. M. M. de Campos, F. P. Barreto, A. S. Stender, F. F. Arraes, and V. R. Rosa, "Model based production optimization applied to offshore fields," presented at the OTC Brasil, Rio de Janeiro, Brazil, Oct. 2013, Paper no. OTC-24301-MS, doi: 10.4043/24301-MS.

[4] B. Foss, B. R. Knudsen, and B. Grimstad, "Petroleum production optimization—A static or dynamic problem?" *Comput. Chem. Eng.*, vol. 114, pp. 245–253, Jun. 2018, doi: 10.1016/j.compchemeng.2017.10.009.

[5] A. Pavlov, D. Krishnamoorthy, K. Fjalestad, E. Aske, and M. Fredriksen, "Modelling and model predictive control of oil wells with electric submersible pumps," in *Proc. IEEE Conf. Control Appl. (CCA)*, Juan Les Antibes, France, Oct. 2014, pp. 586–592.

[6] B. J. T. Binder, D. K. M. Kufoalor, A. Pavlov, and T. A. Johansen, "Embedded model predictive control for an electric submersible pump on a programmable logic controller," in *Proc. IEEE Conf. Control Appl. (CCA)*, Juan Les Antibes, France, Oct. 2014, pp. 579–585.

[7] B. J. T. Binder, A. Pavlov, and T. A. Johansen, "Estimation of flow rate and viscosity in a well with an Electric Submersible Pump using Moving Horizon Estimation," *IFAC-PapersOnLine*, vol. 48, no. 6, pp. 140–146, Jul. 2015, doi: 10.1016/j.ifacol.2015.08.022.

[8] R. Sharma and B. Glemmestad, "Modeling and simulation of an electric submersible pump lifted oil field," *Int. J. Petroleum Sci. Technol.*, vol. 8, no. 1, pp. 39–68, 2014.

[9] R. Sharma and B. Glemmestad, "Optimal control strategies with nonlinear optimization for an electric submersible pump lifted oil field," *Model., Identificat. Control*, vol. 34, no. 2, pp. 55–67, 2013, doi: 10.4173/mic.2013.2.2.

[10] R. Sharma and S. Glemmestad, "Mixed integer nonlinear optimization for ESP lifted oil field and improved operation through production valve choking," *Int. J. Model. Optim.*, vol. 4, no. 6, pp. 465–475, Dec. 2014, doi: 10.7763/IJMO.2014.V4.419.

[11] R. Sharma and B. Glemmestad, "Nonlinear model predictive control for optimal operation of electric submersible pump lifted oil field," in *Proc. Model., Identificat. Control*, Innsbruck, Austria, 2014, pp. 229–236.

[12] D. Krishnamoorthy, E. M. Bergheim, A. Pavlov, M. Fredriksen, and K. Fjalestad, "Modelling and robustness analysis of model predictive control for electrical submersible pump lifted heavy oil wells," *IFAC-PapersOnLine*, vol. 49, no. 7, pp. 544–549, 2016, doi: 10.1016/j.ifacol.2016.07.399.

[13] P. D. A. Delou, J. P. A. de Azevedo, D. Krishnamoorthy, M. B. de Souza, and A. R. Secchi, "Model predictive control with adaptive strategy applied to an Electric Submersible Pump in a subsea environment," *IFAC-PapersOnLine*, vol. 52, no. 1, pp. 784–789, 2019, doi: 10.1016/j.ifacol.2019.06.157.

[14] B. A. Santana, R. M. Fontes, L. Schnitman, and M. A. F. Martins, "An adaptive infinite horizon model predictive control strategy applied to an ESP-lifted oil well system," *IFAC-PapersOnLine*, vol. 54, no. 3, pp. 176–181, 2021, doi: 10.1016/j.ifacol.2021.08.238.

[15] B. J. T. Binder, T. A. Johansen, and L. Imsland, "Improved predictions from measured disturbances in linear model predictive control," *J. Process Control*, vol. 75, pp. 86–106, Mar. 2019, doi: 10.1016/j.jprocont.2019.01.007.

[16] E. A. Costa, O. S. L. D. Abreu, T. D. O. Silva, M. P. Ribeiro, and L. Schnitman, "A Bayesian approach to the dynamic modeling of ESP-lifted oil well systems: An experimental validation on an ESP prototype," *J. Petroleum Sci. Eng.*, vol. 205, Oct. 2021, Art. no. 108880, doi: 10.1016/j.petrol.2021.108880.

[17] R. M. Fontes, D. D. Santana, and M. A. F. Martins, "An MPC auto-tuning framework for tracking economic goals of an ESP-lifted oil well," *J. Petroleum Sci. Eng.*, vol. 217, Oct. 2022, Art. no. 110867, doi: 10.1016/j.petrol.2022.110867.

[18] J. P. Jordanou, I. Osnes, S. B. Hernes, E. Camponogara, E. A. Antonelo, and L. Imsland, "Nonlinear model predictive control of electrical submersible pumps based on echo state networks," *Adv. Eng. Informat.*, vol. 52, Apr. 2022, Art. no. 101553, doi: 10.1016/j.aei.2022.101553.

[19] N. Janatian, K. Jayamanne, and R. Sharma, "Model based control and analysis of gas lifted oil field for optimal operation," in *Proc. 1st SIMS EUROSIM Conf. Model. Simulation*, Mar. 2022, pp. 241–246.

[20] N. Janatian and R. Sharma, "Multi-stage scenario-based MPC for short term oil production optimization under the presence of uncertainty," *J. Process Control*, vol. 118, pp. 95–105, Oct. 2022, doi: 10.1016/j.jprocont.2022.08.012.

[21] S. Lucia, T. Finkler, and S. Engell, "Multi-stage nonlinear model predictive control applied to a semi-batch polymerization reactor under uncertainty," *J. Process Control*, vol. 23, no. 9, pp. 1306–1319, Oct. 2013, doi: 10.1016/j.jprocont.2013.08.008.

[22] M. A. Nasab, M. Zand, S. Padmanaban, M. S. Bhaskar, and J. M. Guerrero, "An efficient, robust optimization model for the unit commitment considering renewable uncertainty and pumped-storage hydropower," *Comput. Electr. Eng.*, vol. 100, May 2022, Art. no. 107846, doi: 10.1016/j.compeleceng.2022.107846.

[23] D. Krishnamoorthy, B. Foss, and S. Skogestad, "Real-time optimization under uncertainty applied to a gas lifted well network," *Processes*, vol. 4, no. 4, p. 52, Dec. 2016, doi: 10.3390/pr4040052.

[24] N. Janatian, and R. Sharma, "A robust model predictive control with constraint modification for gas lift allocation optimization," *J. Process Control*, vol. 128, Aug. 2023, Art. no. 102996, doi: 10.1016/j.jprocont.2023.102996.

[25] G. Takacs, *Electrical Submersible Pumps Manual: Design, Operations, and Maintenance* Cambridge, MA, USA: Gulf, 2017, pp. 11–52.

[26] T. Serghides, "Estimate friction factor accurately," *Chem. Eng. J.*, vol. 91, no. 5, pp. 63–64, 1984.

NIMA JANATIAN received the B.S. and M.S. degrees in mechanical engineering from the Amirkabir University of Technology, Tehran, in 2013 and 2016, respectively. He is currently pursuing the Ph.D. degree in process energy and automation engineering with the University of South-Eastern Norway, Porsgrunn. His research interests include advanced model-based control, robust model predictive control, and real-time optimization under uncertainty with application to energy systems.

ROSHAN SHARMA received the B.S. degree in engineering from Tribhuvan University, Kirtipur, in 2007, and the M.S. degree in systems and control engineering and the Ph.D. degree in process, energy and automation engineering from the Telemark University College, Norway, in 2011 and 2014, respectively. After about two years of academic experience as an assistant lecturer, he received his M.S. and Ph.D. degrees. He is currently an Associate Professor with the University of South-Eastern Norway, Porsgrunn. His research interests include advanced process control and optimization.

• • •